



Cell adhesion proteins in the cerebrospinal fluid of neonates prenatally exposed to Zika virus: A case-control study

Clara L. Ramos¹ | Eduardo C. Nascimento-Carvalho¹ |
 Gustavo C. Nascimento-Carvalho¹ | Martijn M. VanDuijn²  |
 Ana-Luisa Vilas-Boas¹ | Otávio A. Moreno-Carvalho³ | Lucas P. Carvalho⁴ |
 Lona Zeneyedpour² | Gerben Ferwerda⁵ | Ronald de Groot⁵ |
 Theo M. Luider² | Cristiana M. Nascimento-Carvalho⁶ 

¹Bahiana Foundation for Science Development, Bahiana School of Medicine, Salvador, Brazil

²Department of Neurology, Erasmus MC, Rotterdam, Netherlands

³Cerebrospinal Fluid Laboratory, José Silveira Foundation, Salvador, Brazil

⁴Laboratory of Clinical Research, LAPEC, Gonçalves Moniz Institute, Salvador, Brazil

⁵Section of Paediatric Infectious Diseases, Laboratory of Medical Immunology, Radboud Institute for Molecular Life Sciences, Radboud Centre for Infectious Diseases, Radboud University Medical Center, Nijmegen, Netherlands

⁶Department of Paediatrics, Federal University of Bahia School of Medicine, Salvador, Brazil

Correspondence

Cristiana M. Nascimento-Carvalho,
 Department of Paediatrics, Federal
 University of Bahia School of Medicine,
 Rua Prof. Aristides Novis, 105/1201B,
 Salvador 40210-630, Brazil.
 Email: nascimentocarvalho@hotmail.com

Funding information

This research was sponsored by the Brazilian Council for Scientific and Technological Development (Conselho

Abstract

To compare cell adhesion molecules levels in cerebrospinal fluid (CSF) between Zika virus (ZIKV)-exposed neonates with/without microcephaly (cases) and controls, 16 neonates (cases), 8 (50%) with and 8 (50%) without microcephaly, who underwent lumbar puncture (LP) during the ZIKV epidemic (2015–2016) were included. All mothers reported ZIKV clinical symptoms during gestation, all neonates presented with congenital infection findings, and other congenital infections were ruled out. Fourteen control neonates underwent LP in the same laboratory (2017–2018). Five cell adhesion proteins were measured in the CSF using mass spectrometry. Neurexin-1 (3.50 [2.00–4.00] vs. 7.5 [5.00–10.25], $P = 0.001$), neurexin-3 (0.00 [0.00–0.00] vs. 3.00 [1.50–4.00], $P = 0.001$) and neural cell adhesion molecule 2 (NCAM2) (0.00 [0.00–0.75] vs. 1.00 [1.00–2.00], $P = 0.001$) were significantly lower in microcephalic and non-microcephalic cases than in controls. When these two sub-groups of prenatally ZIKA-exposed children were compared to controls separately, the same results were found. When cases with and without microcephaly were compared, no difference was found. Neurexin-3 (18.8% vs. 78.6%, $P = 0.001$) and NCAM2 (25.0% vs. 85.7%, $P = 0.001$) were less frequently found among the cases. A positive correlation was found between cephalic perimeter and levels of these two proteins. Neurexin-2 and neurexin-2b presented no significant differences. Levels of three cell adhesion proteins were significantly lower in CSF of neonates exposed to ZIKV before birth than in controls, irrespective of presence of congenital microcephaly. Moreover, the

Abbreviations: CNS, central nervous system; CSF, cerebrospinal fluid; GOT, oxaloacetic transaminase; IQR, interquartile range; LDH, lactate dehydrogenase; LP, lumbar puncture; MS/MS, mass spectrometry; NCAM2, neural cell adhesion molecule 2; RBC, red blood cell; SPSS, Statistical Package for the Social Sciences; STORCH-HIV-HTLV-HB-HC, cytomegalovirus, herpes, hepatitis B and C, HIV, HTLV, rubella, syphilis, toxoplasmosis; WBC, white blood cell; ZIKV, Zika virus.

Nacional de Desenvolvimento Científico e Tecnológico, CNPq) (grant number 313466/2018-1). Clara L. Ramos received research fellowship from the Bahia State Research Support Foundation. Cristiana M. Nascimento-Carvalho is a senior researcher at the CNPq, Brazil.

smaller the cephalic perimeter, the lower CSF cell adhesion protein levels. These findings suggest that low CSF levels of neurexin-1, neurexin-3 and NCAM2 may reflect the effects of ZIKV on foetal brain development.

KEYWORDS

cell adhesion protein, cerebrospinal fluid, congenital Zika virus infection, mass spectrometry, microcephaly

1 | INTRODUCTION

Brazil was the epicentre of the Zika virus (ZIKV) outbreak in 2015 (Zanluca et al., 2015). Initially, it was considered a self-limited and benign Flavivirus infection (Heang et al., 2012), but the inexplicable and unexpected increase in cases of neonates with microcephaly was subsequently associated with ZIKV infection during pregnancy (Mlakar et al., 2016; Rasmussen et al., 2016). Positive tropism between ZIKV and neuronal cells has been demonstrated to affect different levels of neural progenitor cell development, culminating in cell death and consequent tissue damage (Garcez et al., 2016; Li et al., 2016). Therefore, ZIKV plays an important role in disturbing central nervous system (CNS) development during foetal life (Gharbaran & Somenarain, 2019).

Although recent studies have focused on understanding ZIKV-associated neuropathology, there remain gaps, mainly because access to foetal brain tissue does not exist for ethical reasons. Cerebrospinal fluid (CSF), an important biomarker of neurodegenerative diseases, can be an important source of information about biochemical processes in the brain and blood–brain barrier function (Gobom, 2015). Additionally, CSF proteins may help understand disease progression (Gobom, 2015). A recent study including ZIKV-exposed neonates before birth showed that those with microcephaly and abnormal neuroimaging findings were born with significantly higher levels of CSF proteins compared to neonates born without microcephaly or abnormal neuroimaging findings (Ramos et al., 2018). Significantly higher levels of IgM and IgA classes were found in the CSF of neonates exposed to ZIKV before birth than in controls (Nascimento-Carvalho et al., 2020). Thus, an in-depth study of the CSF components is important to understand the neurological manifestations in this group of patients.

Cell adhesion molecules are important for neural development and brain function and morphology (Togashi et al., 2009). In addition, it seems that cell adhesion molecules participate in the migration of immune cells across the blood–brain barrier (Birkner et al., 2019). Despite the advancements in the ZIKV microcephaly-associated field, the profile of CNS cell

adhesion proteins in the CSF after ZIKV exposure has not yet been investigated. Here, we compared the levels of cell adhesion proteins in the CSF of neonates exposed to ZIKV before birth, with or without microcephaly (cases), and those of neonates who were not exposed to ZIKV before birth, with no congenital infection or microcephaly (controls).

2 | PATIENTS AND METHODS

2.1 | Patients

In this ambispective investigation conducted in the CSF Laboratory, in Salvador, Brazil, patients were included as either cases or controls.

We identified cases during the ZIKV outbreak in Brazil (from December 2015 to March 2016) when lumbar puncture (LP) was performed due to the following reasons: (1) congenital infection characteristics, (2) the respective mother complaining of ZIKV infection symptoms (arthralgia, fever, myalgia and rash) during pregnancy and (3) negative laboratory tests for other congenital infections (cytomegalovirus, herpes, hepatitis B and C, HIV, HTLV, rubella, syphilis and toxoplasmosis [STORCH-HIV-HTLV-HB-HC]). All cases met these three inclusion criteria. Congenital microcephaly was defined as cephalic perimeter ≤ 31.9 cm (for male) and ≤ 31.5 cm (for female) for neonates with gestational age ≥ 37 weeks and a cephalic perimeter above 2 standard deviations under mean for neonates with gestational age < 37 weeks (de Souza Campos Fernandes et al., 2016; Passemard et al., 2013).

Controls were selected between November 2017 and September 2018 based on the following inclusion criteria: (1) Their mothers denied ZIKV symptoms during pregnancy, and (2) there was no CNS illness, microcephaly or clinical/laboratory finding of any congenital infection. The control neonates were tapped for other medical reasons. The CSF inclusion criteria for the control group were as follows: (1) age < 5 days, (2) CSF white blood cell (WBC) count $< 9/\text{mm}^3$, (3) CSF protein level < 133 mg/dl and (4) CSF red blood cell (RBC) count $< 1,001$ cells/

mm³. All controls met the six items of the clinical and CSF inclusion criteria described in this section.

In the CSF Laboratory logbook, potential cases and controls were identified immediately after LP had been performed. LP was requested at the discretion of the assistant paediatrician. Subsequently, written informed consent was obtained, medical charts were revised and mothers were asked about prenatal and neonatal data. Results from laboratory tests to investigate congenital infections (STORCH-HIV-HTLV-HB-HC) from all mothers and children were sought, in addition to details about the date of birth (to calculate age when LP was performed), sex, weight, length of gestation, 5-min Apgar score, cephalic perimeter and neuroimaging evaluation.

2.2 | Laboratory analysis in Brazil

In Salvador, Brazil, all CSF samples (from 16 cases and 14 controls) were analysed for routine testing, including the following: (1) evaluation of total cell count (using a Fuchs–Rosenthal chamber), (2) calculation of cytomorphological percentage (using an accelerated gravitational sedimentation technique along with Leishman and Wright staining) and (3) assessment of protein (using the trichloroacetic acid method), glutamic oxaloacetic transaminase (GOT) (UI/dL) and lactate dehydrogenase (LDH) (UI/L) (both using the colorimetric method) and glucose (determined by the enzymatic method according to Trinder) levels. Serological tests performed on all samples were immunofluorescence (toxoplasmosis), haemagglutination (syphilis and toxoplasmosis), fluorescent treponemal antibody absorption test and Venereal Disease Research Laboratory test. Ziehl–Neelsen stain, Gram stain, Indian ink and latex were used to search for *Streptococcus pneumoniae*; *Haemophilus influenzae*; *Neisseria meningitidis* A, B and C; and *Cryptococcus neoformans* antigens. Every sample was incubated to isolate aerobic pyogenic bacteria, mycobacteria and fungi. A comparison of CSF results between cases and controls has been previously published (Nascimento-Carvalho et al., 2020). The residual CSF samples were kept frozen at -20°C and were shipped to the Laboratory of Neuro-Oncology, Department of Neurology/Clinical & Cancer Proteomics, Erasmus MC, Rotterdam, the Netherlands, by airplane at the same temperature.

2.3 | Proteomics analysis in the Netherlands

It is important to highlight that proteomics measurements aim to identify all proteins contained in the CSF

samples. Blinding of laboratory procedures was guaranteed, as each sample was identified by a random number. All the solvents were purchased from Biosolve (Valkenswaard, the Netherlands). The CSF samples were digested according to a previously published method (Nascimento-Carvalho et al., 2020). Briefly, 20 μl of CSF was digested with trypsin (Promega, Madison, WI, USA) after reduction and alkylation with dithiothreitol (Sigma-Aldrich, Saint Louis, MO, USA) and iodoacetamide (Sigma-Aldrich, Saint Louis, MO, USA). Samples were analysed using a nano-LC (Ultimate 3000RS, Thermo Fisher Scientific, Germering, Germany). After the pre-concentration and washing of the samples on a C18 trap column (5 mm \times 300 μm i.d., Thermo Fisher Scientific), each sample was loaded onto a C18 column (PepMap C18, 75 m ID \times 250 mm, 2- μm particle, and 100 \AA pore size; Thermo Fisher Scientific) using a linear 90-min gradient (4–38% of 80% ACN/H₂O, 0.08% formic acid) at a flow rate of 300 nl/min. Orbitrap Fusion Lumos (Thermo Fisher Scientific, San Jose, CA, USA) with a nanospray source was coupled to a nano-LC, and the mode of operation was data-dependent acquisition.

Mass spectrometry (MS/MS) spectra were extracted from the data files and transformed into MGF files using ProteoWizard MS Convert (version 3.0.10444). The MGF files were analysed using Mascot (version 2.3.02; Matrix Science Inc., London, UK). Mascot was used to search for the human subset of the UniProt/Swiss-Prot 2015_11 database, *Homo sapiens* species restriction and 20,194 sequences of the extracted MS/MS data. For this database search, the following settings were used: up to two missed cleavages, oxidation as a variable modification of methionine and carbamidomethylation as a fixed change of cysteine. The enzyme used was trypsin. A peptide mass tolerance of up to 10 ppm and 0.02 Da of fragment mass tolerance were accepted. To summarise and filter MS/MS-based peptides and protein identification at a false discovery rate of 1% (peptide level), the Scaffold software (version 4.8.7, Proteome software, Portland, OR, USA) was used. Proteins with similar peptides that could not be distinguished by MS/MS analysis alone were categorised together. Overall, 409 proteins (526 with open clusters) were identified and quantified. The complete list of these 409 proteins is presented in Table S1 (Excel database format), and the unique peptides identified in these proteins are listed.

2.4 | Data entry and analysis

We used the QuickGO platform to identify the proteins that were cell-adhesion molecules among the 409 different proteins quantified in the CSF. QuickGO allows us to

navigate through a large database involving the Gene Ontology (GO) (Binns et al., 2009). It provides three main characteristics related to gene products regarding the molecular functions and biological processes in which they are compelled and where they are located in a cell structure (Binns et al., 2009). GO plays an important role in proteomics and genomics datasets (Dimmer et al., 2008). QuickGO can provide protein data from UniProtKB based on selected categories (Binns et al., 2009). The categories were filled as follows: Taxon: *H. sapiens*, Gene Products: Proteins, GO terms: neuron cell–cell adhesion and Aspects: Biological Process. Subsequently, a list of neuron cell–cell adhesion proteins was imported from GO annotation using the QuickGO (www.ebi.ac.uk/QuickGO/annotations?taxonId=9606&taxonUsage=exact&goId=GO:0007158&goUsageRelationships=is_a,part_of,occurs_in&goUsage=descendants&geneProductSubset=Swiss-Prot&geneProductType=protein&aspect=biological_process). As a result, an initial list of 37 annotations was found, which resulted in 20 different proteins (Table 1), of which the following five (among all 409 proteins) were quantified in the CSF samples studied in this investigation: neurexin-1, neurexin-2, neurexin-2

beta, neurexin-3 and neural cell adhesion molecule 2 (NCAM2). In this study, we reported the results of the analysis of these five cell adhesion proteins detected and quantified in the CSF samples, which were the five proteins found in the CSF samples of the 20 different neuron cell–cell adhesion proteins retrieved from the GO annotation on the QuickGO platform.

Data entry into the Statistical Package for the Social Sciences (SPSS, version 9.0) was verified. Subsequently, analysis was performed. The results of the five cell adhesion protein levels found in the CSF samples are presented as median values with the respective interquartile range (IQR) owing to an apparent non-parametric distribution. The Mann–Whitney U test was used to compare the median (IQR) between the two groups. The correlation between cell adhesion protein levels in the CSF and cephalic perimeter was assessed using Spearman's test. Pearson's chi-squared test and Fisher's exact test, as appropriate, were used to compare categorical variables, which comprised the presence or absence of each protein in each CSF sample (results presented as percentages). Boxplot graphs were drawn in SPSS to graphically present the levels of the five cell adhesion molecules found and quantified in the CSF samples. The results were categorised as cases or controls, and cases were grouped into microcephalic and non-microcephalic neonates. Dispersion graphs were drawn in Excel software to graphically present the levels of the cell adhesion molecules correlated with cephalic perimeter, and the square of the correlation (R^2) is presented to demonstrate the proportion of variation in the dependent variables (neurexin-3 and NCAM2), which can be attributed to the independent variable (cephalic perimeter). All tests were two-tailed, and statistical significance was considered when P was <0.05 . The criteria to include controls aimed to ensure that cases and controls would have similar characteristics, except for having been prenatally exposed to ZIKV.

TABLE 1 List of neuron cell–cell adhesion proteins imported from gene ontology annotation by QuickGo platform

Protein	Gene
Astrotactin-1	ASTN1
Neural cell adhesion molecule 2	NCAM2
Astrotactin-2	ASTN2
Proto-oncogene tyrosine-protein kinase receptor Ret	RET
Bile salt-activated lipase	CEL
Neurexin-1-beta	NRXN1
Neurexin-2-beta	NRXN2
Cyclin-dependent kinase 5 activator 1	CDK5R1
Contactin-4	CNTN4
Neurologin-4, X-linked	NLGN4X
Neurologin-1	NLGN1
Neurologin-4, Y-linked	NLGN4Y
Neurologin-2	NLGN2
Tenascin-R	TNR
Neurexin-3-beta	NRXN3
Neurologin-3	NLGN3
Ninjurin-2	NINJ2
Neurexin-2	NRXN2
Neurexin-1	NRXN1
Neurexin-3	NRXN3

2.5 | Ethical aspects

All procedures were performed in accordance with the ethical standards laid down in the 1964 Declaration of Helsinki and its later amendments. This study was approved by the Federal University of Bahia Ethics Committee (approval number: 2.414.857). In the beginning of the interviews, informed consent was obtained from the mothers.

3 | RESULTS

During the ZIKV outbreak in Brazil (from December 2015 to March 2016), for this study, we selected

16 neonates with foetal exposure to ZIKV, 8 (50%) with microcephaly and 8 (50%) without microcephaly, which comprised the case group of this study. Exposure to toxic

substances and drugs, ionising injury and prenatal and perinatal complications that could have caused microcephaly were excluded. Overall, 85 neonates selected as

TABLE 2 Characteristics of 16 cases and 14 controls

Characteristic	Cases (<i>n</i> = 16)	Controls (<i>n</i> = 14)
Prenatal care	16 (100.0%)	14 (100.0%)
Girls	10 (62.5%)	10 (71.4%)
Premature	3 (18.8%) 32w, 33w, 35w ^a	4 (28.6%) 27w, 29w, 32w, 34w ^a
Microcephaly	8 (50.0%)	0
Minimal 5-min Apgar	8	7
Head neuroimaging performance	15 (93.8%)	7 (50.0%)
Head neuroimaging abnormal findings ^b	10 (62.5%)	0
Median (interquartile range) age (days)	2 (1–3) oldest 4	3 (1–4) oldest 4

^aGestational age in weeks.

^bAbnormal findings include calcifications, ventriculomegaly, decreased brain volume, lissencephaly, agenesis of corpus callosum, Dandy-Walker malformation, craniofacial disproportion, periventricular hyperechogenicity, subependymal cyst, cortex-subcortical indistinction, enlarged cisterna magna.

TABLE 3 Routine cerebrospinal fluid parameters of 16 cases and 14 control neonates

Characteristic median (interquartile range)	Cases (<i>n</i> = 16)	Controls (<i>n</i> = 14)
CSF white blood cell/mm ³	3.2 (0.4–8.7)	1.2 (0.7–2.9)
% lymphocyte	50.0 (45.3–57.0)	58.0 (50.8–65.8)
% monocyte	48.0 (42.3–51.8)	41.0 (34.3–46.5)
% macrophage	2.0 (0.0–3.0)	1.0 (0.0–1.0)
% neutrophil	0	0
Protein (mg/dl)*	127.5 (86.8–154.0)	64.5 (49.5–80.5)
Chloride (mg/dl)	695.5 (694–700)	694 (686–697)
Glucose (mg/dl)	39.5 (30.5–44.3)	39.0 (30.8–51.8)
GOT (UI/dL)**	5.8 (4.5–8.8)	3.7 (3.7–4.5)
LDH (UI/L)***	60.2 (43.2–71.6)	39.2 (36.2–46.2)

Note: CSF White blood cell/mm³ by using a Fuchs-Rosenthal chamber. Cytomorphological percentage using an accelerated gravitational sedimentation technique along with Leishman and Wright staining. Protein amount (mg/dl) using the trichloroacetic acid method. Glucose amount (mg/dl) determined by the enzymatic method according to Trinder. Glutamic oxalacetic transaminase (GOT) (UI/dl) and lactic dehydrogenase (LDH) (UI/L) measurement using the colorimetric method.

**p* < 0.001 (Mann–Whitney U test).

***p* = 0.001 (Mann–Whitney U test).

****p* = 0.003 (Mann–Whitney U test).

TABLE 4 Comparison of median (interquartile range) of cell adhesion proteins levels (number of unique peptides) in the cerebrospinal fluid (CSF) of control neonates with and without red blood cells (RBC) in the CSF

CSF cell adhesion protein	Controls without RBC <i>n</i> = 10	Controls with RBC <i>n</i> = 4	<i>p</i>
Neurexin-1	7.50 (5.00–11.00)	6.50 (2.75–9.50)	0.5
Neurexin-3	3.00 (1.50–4.00)	2.50 (0.50–3.75)	0.7
Neural cell adhesion molecule 2	1.00 (1.00–2.25)	1.00 (0.25–1.75)	0.5
Neurexin-2	4.00 (3.00–6.00)	3.00 (1.50–6.75)	0.2
Neurexin-2 beta	0.00 (0.00–0.00)	1.50 (0.00–3.00)	0.1

candidates for controls were identified between 23 November 2017 and 30 September 2018. Initially, 45 were excluded due to age ≥ 5 days, 19 due to CSF WBC count $\geq 9/\text{mm}^3$, 9 due to CSF protein $\geq 133 \text{ mg/dl}$, 8 due to CSF RBC count $\geq 1,001/\text{mm}^3$ and 1 due to ventricular tap. Subsequently, 24 patients were found to be potentially eligible for inclusion in the control group. After the mothers were interviewed and data were retrieved from medical records, 10 (41.7%) of these candidates were excluded, as nine mothers had untreated syphilis and one neonate had CNS haemorrhage. Finally, 14 neonates were identified and included as controls, among whom 10 had no RBC in the CSF and four had, 320, 350, 600 and 933 RBC/ mm^3 in the CSF, respectively. The reasons for tapping were as follows: six neonates due to sepsis, five neonates due to treated maternal syphilis, one neonate due to fever without a source, one neonate due to seizure and one neonate due to maternal acute cytomegalovirus infection. Results of serological tests for syphilis from the five neonates at risk of congenital syphilis were negative, both in serum and CSF, whereas the neonate at risk of congenital cytomegalovirus infection had a negative result of the cytomegalovirus polymerase chain reaction in urine during the first week of life. Thus, we selected 30 neonates (16 cases and 14 controls), and their characteristics are shown in Table 2. It is possible to observe that the oldest neonates were 4 days old in both groups and that all mothers received prenatal care. All neonates were born in the maternity units. The routine tests performed in the CSF are shown in Table 3 and grouped into the case and control groups. It is possible to observe that the protein level is twofold higher in the case group than in the control group, which has already been published (Nascimento-Carvalho et al., 2020).

In order to proceed, the CSF levels of the five cell adhesion proteins found in our samples were compared between 10 controls without RBC and 4 controls with RBC (Table 4), and no significant difference was found among these control subgroups. Therefore, controls with and without RBC were grouped together in the control group for subsequent analyses. Cell adhesion protein levels were compared between cases and controls, and the results are shown in Table 5. The (IQR) medians of neurexin-1, neurexin-3 and NCAM2 were significantly lower when neonates with or without microcephaly were grouped together (cases) and compared to controls; similarly, these three molecules presented significantly lower levels when cases with microcephaly were compared to controls and when cases without microcephaly were compared to controls separately. However, when cases with or without microcephaly were compared, no significant difference was found. No difference was found in the levels of neurexin-2 and neurexin-2b when all cases

TABLE 5 Comparison of median (interquartile range) of cell adhesion proteins levels (number of unique peptides) in the cerebrospinal fluid of neonates exposed to ZIKV before birth, with or without congenital microcephaly, and controls

CSF cell adhesion protein	Controls $n = 14$	All cases with and without microcephaly $n = 16$	p^a	Cases with microcephaly $n = 8$	p^b	Cases without microcephaly $n = 8$	p^c	p^d
Proteins with significant difference between all cases together and controls								
Neurexin-1	7.50 (5.00–10.25)	3.50 (2.00–4.00)	0.001	2.00 (1.25–4.00)	0.002	4.00 (2.25–4.75)	0.008	0.3
Neurexin-3	3.00 (1.50–4.00)	0.00 (0.00–0.00)	0.001	0.00 (0.00–0.00)	0.003	0.00 (0.00–1.50)	0.03	0.5
Neural cell adhesion molecule 2	1.00 (1.00–2.00)	0.00 (0.00–0.75)	0.001	0.00 (0.00–0.00)	0.002	0.00 (0.00–1.00)	0.01	0.3
Proteins without significant difference between all cases together and controls								
Neurexin-2	4.00 (3.00–6.00)	3.00 (1.25–4.00)	0.08	3.00 (1.00–4.00)	0.1	3.00 (2.25–4.00)	0.2	0.7
Neurexin-2 beta	0.00 (0.00–0.75)	0.00 (0.00–0.00)	90.0	0.00 (0.00–0.00)	0.2	0.00 (0.00–0.00)	0.2	1.0

^aComparison between 16 cases and 14 controls.

^bComparison between 8 cases with microcephaly and 14 controls.

^cComparison between 8 cases without microcephaly and 14 controls.

^dComparison between 8 cases with and 8 cases without microcephaly.

were compared to controls, when cases with microcephaly were compared to controls or when cases without microcephaly were compared to controls.

Figure 1 shows the distribution of the levels of the five cell adhesion proteins in the 30 CSF samples studied,

grouped as cases or controls; among the cases, the levels are also presented separately in microcephalic or non-microcephalic cases. Figure 1a–c shows how neurexin-1, neurexin-3 and NCAM2 have significantly lower levels in cases than in controls. It was also possible to observe the

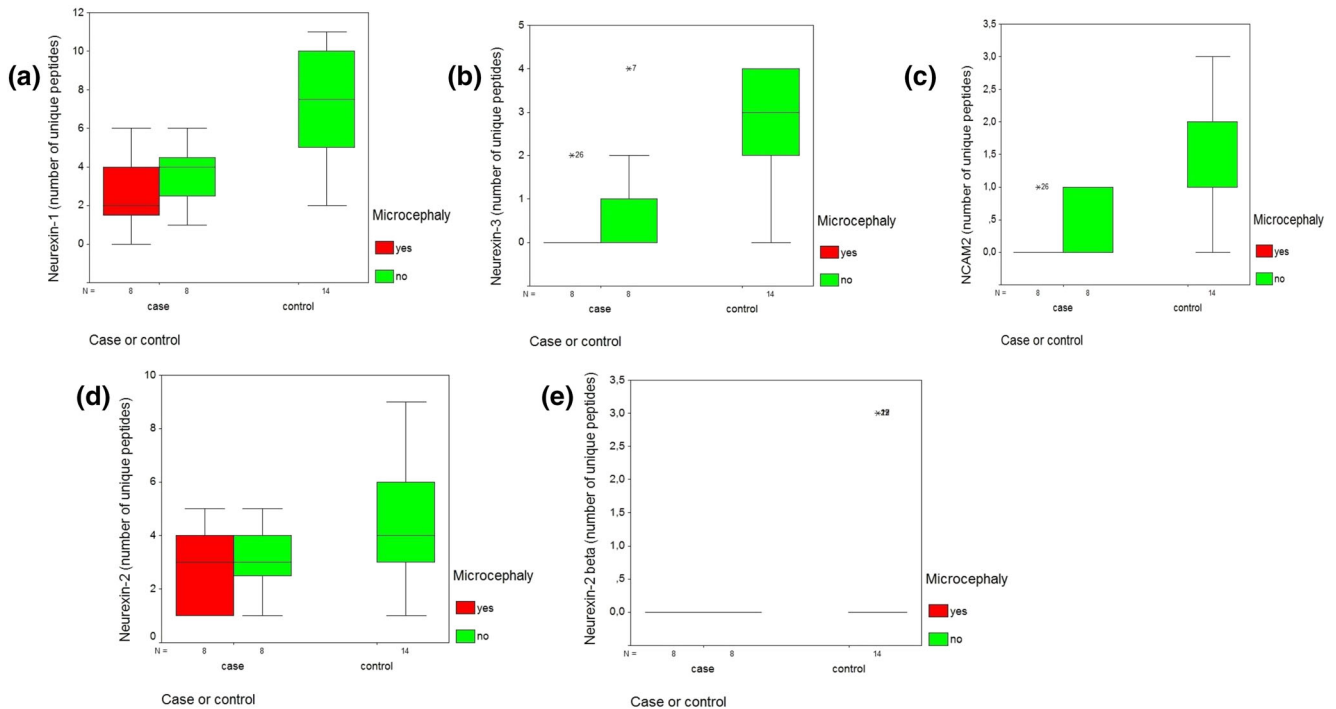


FIGURE 1 Boxplot of the cerebrospinal fluid level of five cell adhesion proteins (a, neurexin-1; b, neurexin-3; c, neural cell adhesion molecule 2; d, neurexin-2; e, neurexin-2 beta) in 16 cases (8 with and 8 without microcephaly) and in 14 control neonates. Graphical presentation of the median (the thick line inside the box), the respective interquartile range (the upper and the lower limit of the box) and of the minimal and maximal values (the upper and the lower limits outside the box) in each subgroup

TABLE 6 Comparison of frequency^a of presence of cell adhesion proteins in the cerebrospinal fluid of neonates exposed to ZIKV before birth, with or without congenital microcephaly, and controls

CSF cell adhesion protein	Controls <i>n</i> = 14	Cases with and without microcephaly <i>n</i> = 16	<i>p</i> ^b	Cases with microcephaly <i>n</i> = 8	<i>p</i> ^c	Cases without microcephaly <i>n</i> = 8	<i>p</i> ^d	<i>p</i> ^e
Neurexin-1	14 (100)	15 (93.8)	1.0 ^f	7 (87.5)	0.4 ^f	8 (100)	-	1.0 ^f
Neurexin-3	11 (78.6)	3 (18.8)	0.001 ^g	1 (12.5)	0.006 ^f	2 (25.0)	0.03 ^f	1.0 ^f
Neural cell adhesion molecule 2	12 (85.7)	4 (25.0)	0.001 ^f	1 (12.5)	0.001 ^f	3 (37.5)	0.5 ^f	0.6 ^f
Neurexin-2	14 (100)	16 (100)	-	8 (100)	-	8 (100)	-	-
Neurexin-2 beta	3 (21.4)	0	0.09 ^f	0	0.3 ^f	0	0.3 ^f	-

^aResults in *n* (%).

^bComparison between 16 cases and 14 controls.

^cComparison between 8 cases with microcephaly and 14 controls.

^dComparison between 8 cases without microcephaly and 14 controls.

^eComparison between 8 cases with and 8 cases without microcephaly.

^fFisher exact test.

^gPearson chi-square.

absence of neurexin-3 and NCAM2 in individual cases. Thus, the measured levels were dichotomised as the presence or absence of each protein, and their frequencies were compared between cases and controls. The absence of neurexin-3 and NCAM2 was significantly higher among the cases (Table 6). On the contrary, neurexin-2 was present in all 30 CSF samples, which means that neurexin-2 was equally present in cases and controls, whereas neurexin-2 beta was only present in three controls and in no cases (Table 6). Figure 1d,e shows graphically these findings.

The assessment of the correlation between the CSF levels of the five cell adhesion proteins and the cephalic perimeter of neonates is shown in Table 7. The correlation was statistically significant and positive for neurexin-3 and NCAM2; that is, the lower the cell adhesion protein level, the smaller the cephalic perimeter. Neurexin-3 and NCAM2 had similar correlation coefficient ($\rho = 0.480$) (Table 7). Figure 2 shows the graphs of correlation between cephalic perimeter and these cell adhesion proteins with significant correlation coefficients (a for neurexin-3 and b for NCAM2).

TABLE 7 Correlation between cell adhesion proteins levels in the cerebrospinal fluid and cephalic perimeter of neonates tapped up to 4 days of life

CSF cell adhesion protein	P	Significant rho
Neurexin-1	0.1	
Neurexin-3	0.007 ^a	0.480
Neural cell adhesion molecule 2	0.007 ^a	0.480
Neurexin-2	0.7	
Neurexin-2 beta	0.8	

^aCorrelation is significant at the 0.01 level (two-tailed).

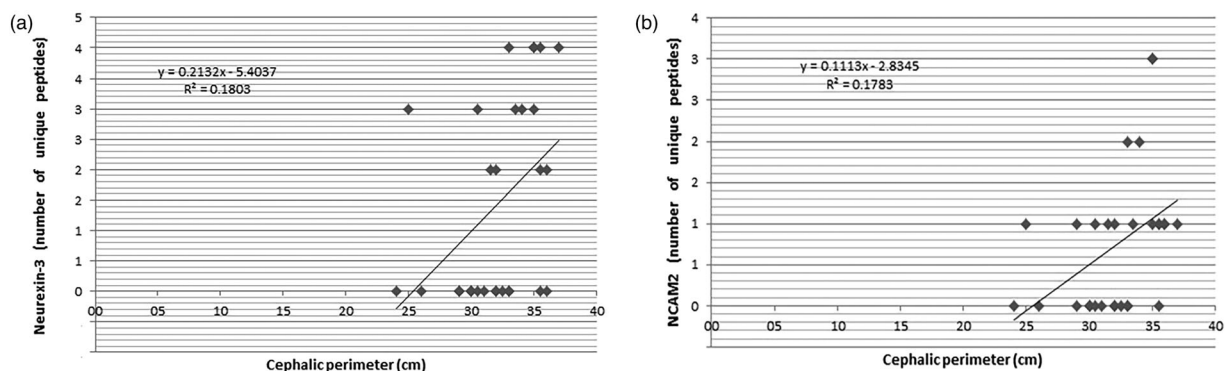


FIGURE 2 Significant positive correlation between cephalic perimeter and two distinct cell adhesion proteins (a, neurexin-3; b, neural cell adhesion molecule 2) levels in the CSF of 30 neonates (y axis: cell adhesion protein level; x axis: cephalic perimeter of the neonates)

4 | DISCUSSION

Notably, the CSF levels of the three cell adhesion proteins were significantly lower in prenatally ZIKV-exposed neonates than in controls, irrespective of the presence of congenital microcephaly. In addition, a positive correlation was found between the cephalic perimeter at birth and the level of the two cell adhesion proteins. Our findings suggest that the low CSF levels of some cell adhesion molecules may reflect the effects of ZIKV on foetal brain development. To the best of our knowledge, this is an innovative finding of this study.

ZIKV can cross the placental barrier and infect the foetus (Quicke et al., 2016). In the brain, ZIKV can reach many neuronal cells (astrocytes and oligodendrocytes) and cause changes in the expression of several cellular genes and proteins (Sher et al., 2019), increase cell death and dysregulate cell cycle progression (Tang et al., 2016). Garcez et al. (2017) used human neurospheres to study molecular pathways caused by the damage of ZIKV infection in the human brain and showed that ZIKV alters cell cycle targets in progenitor cells, induces proliferation arrest, reduces the production of neural cells and induces cell death. For instance, Table 3 shows significantly higher levels of total protein, GOT and LDH among cases compared to controls, which is in accordance with some level of cell death in the CSF of prenatally ZIKV-exposed neonates. As such, it is possible to expect lower levels of some cell adhesion proteins in neonates exposed to ZIKV before birth because of less neural material due to ZIKV damage. Several studies have shown changes in the transcriptomics and proteomics profiles of cells and organisms infected by Influenza viruses (Kobasa et al., 2007; Vester et al., 2009). Recently, several studies have reproduced similar approaches in ZIKV-infected mice or cells in vitro and demonstrated dysregulation (upregulated or

downregulated) in some neuronal proteins (Garcez et al., 2017; Glover et al., 2019; Sher et al., 2019).

Our study found statistically significant differences among the following three neural cell adhesion proteins: neuexin-1, neuexin-3 and NCAM2. Neuexins are a family of cell adhesion molecules that play an important role in synaptic processes (Chen et al., 2017; Quinn et al., 2017). Dysregulation of cell adhesion molecules during brain development may induce structural and functional malformations of brain circuits, resulting in neurological disorders (Yang et al., 2014). Neuexin-1, neuexin-2 and neuexin-3 belong to the neuexin family, and their genetic comparison among members of this family shows greater similarity between neuexin-1 and neuexin-3 in relation to neuexin-2. This suggests that neuexin-2 diverges from a common progenitor of neuexin-1 and neuexin-3 (Südhof, 2017). The neuexin family comprises relevant synaptic adhesion proteins (Camporesi et al., 2022), which have been investigated in the CSF as biomarkers of some psychiatric disorders (al Shweiki et al., 2020; Kasem et al., 2018) and neurodegenerative diseases (Brinkmalm et al., 2018; Hölttä et al., 2015; Zheng et al., 2018), mainly because synaptic dysfunction is primarily observed in these situations. Neuexins are present in synaptic junctions and astrocytes (Trotter et al., 2020). In our study, neuexin-1 and neuexin-3 levels were significantly lower among cases compared to controls, and their genetic similarity may be important to explain why they presented similar results, whereas neuexin-2 and neuexin-2 beta did not differ in such comparison. Rosa-Fernandes et al. (2019) studied human neuro-progenitor cells derived from stem cells and neurones infected with ZIKV; based on proteomic analyses, their study showed dysregulated molecular pathways. In addition, ZIKV infection is associated with downregulation of presynaptic proteins, such as neuexins. In a proteomic analysis, al Shweiki et al. (2020) suggested the feasibility of quantifying synaptic proteins in the CSF, including neuexin-3. There is no evidence of how synaptic proteins can reach the CSF, but given the dynamic process of synapsis (Kondo & Okabe, 2011), decreased levels of these proteins can be related to fewer synapses or synaptic damage that is well cleared from the tissue. The lower levels of neuexins in prenatally ZIKV-exposed neonates may be disruptive to synapsis, which is important for brain development and might contribute to the manifestation of congenital ZIKV syndrome.

NCAM2 is expressed predominantly in the brain and is involved in important neural processes, such as synapsis, axon guidance, proliferation of spinal cord stem cells and neurite outgrowth (Rasmussen et al., 2018; Sheng et al., 2015). Barbeito-Andrés et al. (2020) conducted an experimental study in animal models divided into three

groups based on caloric intake and the presence or absence of a protein deficit. After analysing RNA sequences in the brains of mice on embryonic day 15, they demonstrated that most genes related to neural development, including NCAM2, were downregulated in the group infected with ZIKV, despite the absence of malnutrition. This finding is consistent with that of our study, since lower levels of NCAM2 may be associated with impairment or retardation of normal neural growth and patterning.

More *in vivo* and non-experimental studies in this area are highly required, mainly because most currently available results are based on *in vitro* environments or experimental animal models. In this context, CSF study is important as an indirect measure of brain development. Taking into account the consequences of ZIKV-infected brain, it is possible to infer that the lower level of some cell adhesion proteins in the CSF of prenatally ZIKV-exposed neonates is a consequence of dysregulation of the cell cycle and cell death caused by ZIKV and that the consequences are reflected in the characteristics of congenital ZIKV infection. Such an understanding may be useful for the development of experimental pre-clinical models aimed at the identification of molecules to prevent the extensive damage caused by ZIKV congenital infection in the CNS.

Our study has some limitations. We studied a relatively considerable number of neonates from a medical point of view; however, for statistics, a larger number would provide more confidence. Nonetheless, the compared subgroups were similar to avoid potential confounders. Although serological confirmation of ZIKV infection during pregnancy was missing, we included women with the most common symptoms of ZIKV infection during the outbreak. However, we performed serological tests to exclude other possible congenital infections.

In conclusion, lower levels of some cell adhesion proteins and a positive correlation between cephalic perimeter and CSF cell adhesion protein level may reflect the effects of congenital ZIKV infection in the brain.

ACKNOWLEDGEMENTS

We thank the parents who consented to the interviews and medical record investigations.

CONFLICT OF INTEREST

There is no conflict of interest to be declared.

AUTHOR CONTRIBUTIONS

C.M.N.-C., R.G. and T.M.L. conceived and designed the study. C.L.R., E.C.N.-C., G.C.N.-C., A.-L.V.-B., O.A.M.-C. and L.P.C. included patients, collected samples and performed laboratory tests in Brazil. M.M.VD., L.Z. and G.F. performed the laboratory tests in the Netherlands. All

authors took part in the analysis, wrote the manuscript and contributed intellectual input. All the authors have read and approved the final version of the manuscript.

PEER REVIEW


The peer review history for this article is available at <https://publons.com/publon/10.1111/ejn.15851>.

DATA AVAILABILITY STATEMENT

Datasets used in this study can be requested to the corresponding author.

ORCID

Martijn M. VanDuijn  <https://orcid.org/0000-0002-6654-994X>

Cristiana M. Nascimento-Carvalho  <https://orcid.org/0000-0002-3942-2492>

REFERENCES

- al Shweiki, M. R., Oeckl, P., Steinacker, P., Barschke, P., Dorner-Ciossek, C., Hengerer, B., Schönfeldt-Lecuona, C., & Otto, M. (2020). Proteomic analysis reveals a biosignature of decreased synaptic protein in cerebrospinal fluid of major depressive disorder. *Transl Psychiatry*, *10*(1), 144. <https://doi.org/10.1038/s41398-020-0825-7>
- Barbeito-Andrés, J., Pezzuto, P., Higa, L. M., Dias, A. A., Vasconcelos, J. M., Santos, T. M. P., Ferreira, J. C. C. G., Ferreira, R. O., Dutra, F. F., Rossi, A. D., Barbosa, R. V., Amorim, C. K. N., de Souza, M. P. C., Chimelli, L., Aguiar, R. S., Gonzalez, P. N., Lara, F. A., Castro, M. C., Molnár, Z., ... Garcez, P. P. (2020). Congenital Zika syndrome is associated with maternal protein malnutrition. *Science Advances*, *6*(2), eaaw6284. <https://doi.org/10.1126/sciadv.aaw6284>
- Binns, D., Dimmer, E., Huntley, R., Barrell, D., O'Donovan, C., & Apweiler, R. (2009). QuickGO: A web-based tool for gene ontology searching. *Bioinformatics*, *25*(22), 3045–3046. <https://doi.org/10.1093/bioinformatics/btp536>
- Birkner, K., Loos, J., Gollan, R., Steffen, F., Wasser, B., Ruck, T., Meuth, S. G., Zipp, F., & Bittner, S. (2019). Neuronal ICAM-5 plays a neuroprotective role in progressive neurodegeneration. *Frontiers in Neurology*, *10*, 205. <https://doi.org/10.3389/fneur.2019.00205>
- Brinkmalm, G., Sjödin, S., Simonsen, A. H., Hasselbalch, S. G., Zetterberg, H., Brinkmalm, A., & Blennow, K. (2018). A parallel reaction monitoring mass spectrometric method for analysis of potential CSF biomarkers for Alzheimer's disease. *Proteomics. Clinical Applications*, *12*(1), 1700131. <https://doi.org/10.1002/prca.201700131>
- Camporesi, E., Nilsson, J., Vrillon, A., Cognat, E., Hourregue, C., Zetterberg, H., Blennow, K., Becker, B., Brinkmalm, A., Paquet, C., & Brinkmalm, G. (2022). Quantification of the transsynaptic partners neurexin-neuroligin in CSF of neurodegenerative diseases by parallel reaction monitoring mass spectrometry. *eBioMedicine*, *75*, 103793. <https://doi.org/10.1016/j.ebiom.2021.103793>
- Chen, L. Y., Jiang, M., Zhang, B., Gokce, O., & Südhof, T. C. (2017). Conditional deletion of all neurexins defines diversity of essential synaptic organizer functions for neurexins. *Neuron*, *94*(3), 611–625. <https://doi.org/10.1016/j.neuron.2017.04.011>
- de Souza Campos Fernandes, R. C., de Souza, T. L., & Medina-Acosta, E. (2016). Congenital Zika syndrome in Brazil. *The Lancet Infectious Diseases*, *16*, 772. [https://doi.org/10.1016/S1473-3099\(16\)30079-2](https://doi.org/10.1016/S1473-3099(16)30079-2)
- Dimmer, E. C., Huntley, R. P., Barrell, D. G., Binns, D., Draghici, S., Camon, E. B., Hubank, M., Talmud, P. J., Apweiler, R., & Lovering, R. C. (2008). The gene ontology—Providing a functional role in proteomic studies. *Proteomics*, *8*(23–24). <https://doi.org/10.1002/pmic.200800002>
- Garcez, P. P., Loiola, E. C., Madeiro da Costa, R., Higa, L. M., Trindade, P., Delvecchio, R., Nascimento, J. M., Brindeiro, R., Tanuri, A., & Rehen, S. K. (2016). Zika virus impairs growth in human neurospheres and brain organoids. *Science*, *352*(6287), 816–818. <https://doi.org/10.1126/science.aaf6116>
- Garcez, P. P., Nascimento, J. M., de Vasconcelos, J. M., da Costa, R. M., Delvecchio, R., Trindade, P., Loiola, E. C., Higa, L. M., Cassoli, J. S., Vitória, G., Sequeira, P. C., Sochacki, J., Aguiar, R. S., Fuzii, H. T., de Filippis, A. M. B., Júnior, J. L. S. G. V., Tanuri, A., Martins-de-Souza, D., & Rehen, S. K. (2017). Zika virus disrupts molecular fingerprinting of human neurospheres. *Scientific Reports*, *7*, 40780. <https://doi.org/10.1038/srep40780>
- Gharbaran, R., & Somenarain, L. (2019). Putative cellular and molecular roles of Zika virus in fetal and pediatric neuropathologies. *Pediatric and Developmental Pathology*, *22*(1), 5–21. <https://doi.org/10.1177/1093526618790742>
- Glover, K. K. M., Gao, A., Zahedi-Amiri, A., & Coombs, K. M. (2019). Vero cell proteomic changes induced by Zika virus infection. *Proteomics*, *19*(4), e1800309. <https://doi.org/10.1002/pmic.201800309>
- Gobom, J. (2015). Advancing cerebrospinal fluid biomarker discovery by mass spectrometry. *Neurodegenerative Disease Management*, *5*(5), 371–373. <https://doi.org/10.2217/nmt.15.35>
- Heang, V., Yasuda, C. Y., Sovann, L., Haddow, A. D., Travassos da Rosa, A. P., Tesh, R. B., & Kasper, M. R. (2012). Zika virus infection, Cambodia, 2010. *Emerging Infectious Diseases*, *18*(2), 349–351. <https://doi.org/10.3201/eid1802.111224>
- Hölttä, M., Minthon, L., Hansson, O., Holmén-Larsson, J., Pike, I., Ward, M., Kuhn, K., Rüetschi, U., Zetterberg, H., Blennow, K., & Gobom, J. (2015). An integrated workflow for multiplex CSF proteomics and peptidomics-identification of candidate cerebrospinal fluid biomarkers of Alzheimer's disease. *Journal of Proteome Research*, *14*(2), 654–663. <https://doi.org/10.1021/pr501076j>
- Kasem, E., Kurihara, T., & Tabuchi, K. (2018). Neurexins and neuropsychiatric disorders. *Neuroscience Research*, *127*, 53–60. <https://doi.org/10.1016/j.neures.2017.10.012>
- Kobasa, D., Jones, S. M., Shinya, K., Kash, J. C., Copps, J., Ebihara, H., Hatta, Y., Kim, J. H., Halfmann, P., Hatta, M., Feldmann, F., Alimonti, J. B., Fernando, L., Li, Y., Katze, M. G., Feldmann, H., & Kawaoka, Y. (2007). Aberrant innate immune response in lethal infection of macaques with the 1918 influenza virus. *Nature*, *445*(7125), 319–323. <https://doi.org/10.1038/nature05495>
- Kondo, S., & Okabe, S. (2011). Turnover of synapse and dynamic nature of synaptic molecules in vitro and in vivo. *Acta Histochemica et Cytochemica*, *44*(1), 9–15. <https://doi.org/10.1267/ahc.10035>

- Li, C., Xu, D., Ye, Q., Hong, S., Jiang, Y., Liu, X., Zhang, N., Shi, L., Qin, C. F., & Xu, Z. (2016). Zika virus disrupts neural progenitor development and leads to microcephaly in mice. *Cell Stem Cell*, 19(1), 120–126. <https://doi.org/10.1016/j.stem.2016.04.017>
- Mlakar, J., Korva, M., Tul, N., Popović, M., Poljšak-Prijatelj, M., Mraz, J., Kolenc, M., Rus, K. R., Vipotnik, T. V., Vodusek, V. F., Vizjak, A., Pizem, J., Petrovec, M., & Zupanc, T. A. (2016). Zika virus associated with microcephaly. *The New England Journal of Medicine*, 374(10), 951–958. <https://doi.org/10.1056/NEJMoa1600651>
- Nascimento-Carvalho, G. C., Nascimento-Carvalho, E. C., VanDuijn, M. M., Ramos, C. L., Vilas-Boas, A.-L., Moreno-Carvalho, O. A., Zeneyedpour, L., Ferwerda, G., de Groot, R., Luiders, T. M., & Nascimento-Carvalho, C. M. (2020). Cerebrospinal fluid immunoglobulins are increased in neonates exposed to Zika virus during foetal life. *The Journal of Infection*, 80(4), 419–425. <https://doi.org/10.1016/j.jinf.2020.01.006>
- Passemard, S., Kaindl, A. M., & Verloes, A. (2013). Microcephaly. *Handbook of Clinical Neurology*, 111, 129–141. <https://doi.org/10.1016/B978-0-444-52891-9.00013-0>
- Quicke, K. M., Bowen, J. R., Johnson, E. L., McDonald, C. E., Ma, H., O'Neal, J. T., Rajakumar, A., Wrammert, J., Rimawi, B. H., Pulendran, B., Schinazi, R. F., Chakraborty, R., & Suthar, M. S. (2016). Zika virus infects human placental macrophages. *Cell Host & Microbe*, 20(1), 83–90. <https://doi.org/10.1016/j.chom.2016.05.015>
- Quinn, D. P., Kolar, A., Wigerius, M., Gomm-Kolisko, R. N., Atwi, H., Fawcett, J. P., & Krueger, S. R. (2017). Pan-neurexin perturbation results in compromised synapse stability and a reduction in readily releasable synaptic vesicle pool size. *Scientific Reports*, 7, 42920. <https://doi.org/10.1038/srep42920>
- Ramos, C. L., Moreno-Carvalho, O. A., & Nascimento-Carvalho, C. M. (2018). Cerebrospinal fluid aspects of neonates with or without microcephaly born to mothers with gestational Zika virus clinical symptoms. *The Journal of Infection*, 76(6), 563–569. <https://doi.org/10.1016/j.jinf.2018.02.004>
- Rasmussen, K. K., Falkesgaard, M. H., Winther, M., Roed, N. K., Quistgaard, C. L., Teisen, M. N., Edslev, S. M., Petersen, D. L., Aljubouri, A., Christensen, C., Thulstrup, P. W., Leggio, L. L., Teilmann, K., & Walmod, P. S. (2018). NCAM2 fibronectin type-III domains form a rigid structure that binds and activates the fibroblast growth factor receptor. *Scientific Reports*, 8(1), 8957. <https://doi.org/10.1038/s41598-018-27089-7>
- Rasmussen, S. A., Jamieson, D. J., Honein, M. A., & Petersen, L. R. (2016). Zika virus and birth defects—Reviewing the evidence for causality. *The New England Journal of Medicine*, 374(20), 1981–1987. <https://doi.org/10.1056/NEJMs1604338>
- Rosa-Fernandes, L., Cugola, F. R., Russo, F. B., Kawahara, R., Freire, C. C. M., Leite, P. E. C., Stern, A. C. B., Angeli, C. B., de Oliveira, D. B. L., Melo, S. R., Zanutto, P. M. A., Durigon, E. L., Larsen, M. R., Beltrão-Braga, P. C. B., & Palmisano, G. (2019). Zika virus impairs neurogenesis and synaptogenesis pathways in human neural stem cells and neurons. *Frontiers in Cellular Neuroscience*, 13, 64. <https://doi.org/10.3389/fncel.2019.00064>
- Sheng, L., Leshchyn'ska, I., & Sytnyk, V. (2015). Neural cell adhesion molecule 2 promotes the formation of filopodia and neurite branching by inducing submembrane increases in Ca²⁺ levels. *The Journal of Neuroscience*, 35(4), 1739–1752. <https://doi.org/10.1523/JNEUROSCI.1714-14.2015>
- Sher, A. A., Glover, K. K. M., & Coombs, K. M. (2019). Zika virus infection disrupts astrocytic proteins involved in synapse control and axon guidance. *Frontiers in Microbiology*, 10, 596. <https://doi.org/10.3389/fmicb.2019.00596>
- Südhof, T. C. (2017). Synaptic neurexin complexes: A molecular code for the logic of neural circuits. *Cell*, 171(4), 745–769. <https://doi.org/10.1016/j.cell.2017.10.024>
- Tang, H., Hammack, C., Oden, S. C., Wen, Z., Qian, X., Li, Y., Yao, B., Shin, J., Zhang, F., Lee, E. M., Christian, K. M., Didier, R. A., Jin, P., Song, H., & Ming, G. (2016). Zika virus infects human cortical neural progenitors and attenuates their growth. *Cell Stem Cell*, 18(5), 587–590. <https://doi.org/10.1016/j.stem.2016.02.016>
- Togashi, H., Sakisaka, T., & Takai, Y. (2009). Cell adhesion molecules in the central nervous system. *Cell Adhesion & Migration*, 3(1), 29–35. <https://doi.org/10.4161/cam.3.1.6773>
- Trotter, J. H., Dargaei, Z., Wöhr, M., Liakath-Ali, K., Raju, K., Essayan-Perez, S., Nabet, A., Liu, X., & Südhof, T. C. (2020). Astrocytic neurexin-1 orchestrates functional synapse assembly. *BioRxiv*. DOI: <https://doi.org/10.1101/2020.08.21.262097>
- Vester, D., Rapp, E., Gade, D., Genzel, Y., & Reichl, U. (2009). Quantitative analysis of cellular proteome alterations in human influenza A virus-infected mammalian cell lines. *Proteomics*, 9(12), 3316–3327. <https://doi.org/10.1002/pmic.200800893>
- Yang, X., Hou, D., Jiang, W., & Zhang, C. (2014). Intercellular protein-protein interactions at synapses. *Protein & Cell*, 5(6), 420–444. <https://doi.org/10.1007/s13238-014-0054-z>
- Zanluca, C., Melo, V. C., Mosimann, A. L., Santos, G. I., Santos, C. N., & Luz, K. (2015). First report of autochthonous transmission of Zika virus in Brazil. *Memórias Do Instituto Oswaldo Cruz*, 110(4), 569–572. <https://doi.org/10.1590/0074-02760150192>
- Zheng, J.-J., Li, W.-X., Liu, J.-Q., Guo, Y.-C., Wang, Q., Li, G.-H., Dai, S.-X., & Huang, J.-F. (2018). Low expression of aging-related NRXN3 is associated with Alzheimer disease: A systematic review and meta-analysis. *Medicine (Baltimore)*, 97(28), e11343. <https://doi.org/10.1097/MD.00000000000011343>

SUPPORTING INFORMATION

Additional supporting information can be found online in the Supporting Information section at the end of this article.

How to cite this article: Ramos, C. L., Nascimento-Carvalho, E. C., Nascimento-Carvalho, G. C., VanDuijn, M. M., Vilas-Boas, A.-L., Moreno-Carvalho, O. A., Carvalho, L. P., Zeneyedpour, L., Ferwerda, G., de Groot, R., Luiders, T. M., & Nascimento-Carvalho, C. M. (2022). Cell adhesion proteins in the cerebrospinal fluid of neonates prenatally exposed to Zika virus: A case-control study. *European Journal of Neuroscience*, 56(12), 6258–6268. <https://doi.org/10.1111/ejn.15851>